Blocking protein farnesyltransferase improves nuclear shape in fibroblasts from humans with progeroid syndromes

Julia I. Toth*, Shao H. Yang*, Xin Qiao*, Anne P. Beigneux*, Michael H. Gelb†, Casey L. Moulson‡, Jeffrey H. Miner‡, Stephen G. Young*, and Loren G. Fong*§

*Department of Medicine and Division of Cardiology, David Geffen School of Medicine, University of California, Los Angeles, CA 90095; †Departments of Chemistry and Biochemistry, University of Washington, Seattle, WA 98195; and ‡Department of Medicine and Renal Division, Washington University School of Medicine, St. Louis, MO 63110

Communicated by Richard J. Havel, University of California, San Francisco, CA, July 8, 2005 (received for review June 15, 2005)

Defects in the biogenesis of lamin A from its farnesylated precursor, prelamin A, lead to the accumulation of prelamin A at the nuclear envelope, cause misshapen nuclei, and result in progeroid syndromes. A deficiency in ZMPSTE24, a protease involved in prelamin A processing, leads to prelamin A accumulation, an absence of mature lamin A, misshapen nuclei, and a lethal perinatal progeroid syndrome: restrictive dermopathy (RD). Hutchinson–Gilford progeria syndrome (HGPS) is caused by a mutant prelamin A that cannot be processed to lamin A. The hallmark cellular abnormality in RD and HGPS is misshapen nuclei. We hypothesized that the farnesylation of prelamin A is important for its targeting to the nuclear envelope in RD and HGPS and that blocking farnesylation would ameliorate the nuclear shape abnormalities. Indeed, when RD fibroblasts were treated with a farnesyltransferase inhibitor (FTI), prelamin A was partially mislocalized away from the nuclear envelope, and the frequency of nuclear shape abnormalities was reduced ($P < 0.0001$). A FTI also mislocalized prelamin A and improved nuclear shape in *Zmpste24*-deficient mouse embryonic fibroblasts ($P < 0.0001$) and improved nuclear shape in human HGPS fibroblasts ($P < 0.0001$). Most remarkably, a FTI significantly improved nuclear shape in two fibroblast cell lines from atypical progeria patients with lamin A missense mutations in the absence of prelamin A accumulation ($P = 0.0003$ and $P < 0.0001$). These findings establish a paradigm for ameliorating the most obvious cellular pathology in lamin-related progeroid syndromes and suggest a potential strategy for treating these diseases.

aging | Hutchinson–Gilford progeria syndrome | lamin | restrictive dermopathy | ZMPSTE24

Two progerioid disorders in humans, restrictive dermopathy (RD) and Hutchinson–Gilford progeria syndrome (HGPS), are caused by defective biogenesis of lamin A from prelamin A, a farnesylated precursor protein (1–3). RD is a lethal perinatal progeroid disorder characterized by retarded growth, tight and rigid skin, alopecia, micrognathia, and other bone abnormalities. RD is caused by a deficiency in ZMPSTE24 (1, 2), a protease required for the endoproteolytic processing of prelamin A to mature lamin A (4, 5). HGPS is characterized by retarded growth, partial lipodystrophy, osteoporosis, osteolytic lesions, thin skin, micrognathia, and premature atherosclerosis (3). HGPS is caused by a mutant form of prelamin A (commonly called progerin) that cannot be processed to mature lamin A (3). Lamin A is a key protein within the nuclear lamina, an intermediate filament meshwork lining the inner nuclear membrane that provides structural support for the nucleus (6).

Some progeroid syndromes are caused by missense mutations in *LMNA* (the gene for prelamin A and lamin C) (7, 8). For example, E578V and R644C mutations cause progeroid disorders and are associated with nuclear shape abnormalities (8). In these cases, the structural abnormality in lamin A is apparently sufficient to impair nuclear envelope integrity and cause disease.

Prelamin A terminates with a *CAAX* motif (6), which triggers farnesylation of the cysteine (the *C* of the *CAAX* motif) by protein farnesyltransferase. After farnesylation, the last three amino acids of the protein (i.e., the *AAX* of the *CAAX* motif) are released by an endoprotease (likely a redundant function of RCE1 and ZMPSTE24) (5, 9), and the newly exposed farnesylcysteine is methylated by isoprenylcysteine carboxyl methyltransferase (5). Finally, the last 15 aa of prelamin A (including the farnesylcysteine methyl ester) are clipped off by ZMPSTE24, leaving behind mature lamin A (4, 5, 9). Farnesylation of prelamin A is required for all of the subsequent posttranslational processing steps and is thought to be important for the targeting of prelamin A to the nuclear envelope, where lamin A is probably released (10–12). In the absence of farnesylation, prelamin A reaches the nucleoplasm, but little reaches the nuclear envelope, likely because the farnesylcysteine methyl ester is important for the targeting of the protein to the inner nuclear membrane (10–12).

In HGPS, a point mutation leads to the deletion of 50 aa within the carboxyl terminus of prelamin A (3). This deletion leaves the *CAAX* motif intact and is therefore not expected to affect farnesylation, the release of the *AAX*, or methylation. However, the deletion eliminates the site for the second endoproteolytic cleavage, so the mutant protein (progerin) cannot be processed to lamin A (3). Human HGPS fibroblasts contain grossly misshapen nuclei, which are caused by the accumulation of progerin along the nuclear envelope (13, 14). In *Zmpste24*-deficient fibroblasts (*Zmpste24*$^{-/-}$), prelamin A accumulates at the nuclear envelope (4, 15), causing misshapen nuclei with blebs and herniations of the heterochromatin (4, 15). *Zmpste24*$^{-/-}$ mice manifest a host of progeria-like disease phenotypes, which are clearly caused by an accumulation of farnesyl-prelamin A (15). Human RD fibroblasts, which lack ZMPSTE24, also display prelamin A accumulation and misshapen nuclei (1, 2).

We hypothesized that farnesylation was critical for the targeting of prelamin A to the inner nuclear membrane and that the presence of prelamin A at the nuclear envelope was central to the most striking cellular pathology (i.e., misshapen nuclei). We further hypothesized that blocking protein farnesylation with an farnesyltransferase inhibitor (FTI) would reduce prelamin A targeting to the nuclear lamina and improve nuclear shape. Moreover, we hypothesized that FTIs would be effective in ameliorating nuclear shape abnormalities in progeroid syndromes caused by lamin A missense mutations. In those cases, we suspected that the FTI would improve nuclear shape by blocking lamin A biogenesis and limiting

Freely available online through the PNAS open access option.

Abbreviations: RD, restrictive dermopathy; HGPS, Hutchinson–Gilford progeria syndrome; FTI, protein farnesyltransferase inhibitor; MEFs, mouse embryonic fibroblasts; LAP2, lamina-associated protein 2.

§To whom correspondence should be addressed at: 695 Charles E. Young Dr. South, Los Angeles, CA 90095. E-mail: lfong@mednet.ucla.edu.

the delivery of the mutant lamin A to the nuclear envelope. In the current study, we tested each of these hypotheses.

Materials and Methods

Cell Culture. Primary mouse embryonic fibroblasts (MEFs) were prepared from embryonic day 13.5 *Zmpste24*$^{-/-}$ and *Zmpste24*$^{+/+}$ embryos (5). Human skin fibroblasts from an RD patient and a control subject (American Type Culture Collection no. CCL-110) are described in ref. 1. Human HGPS fibroblasts were obtained from the Coriell Cell Repository (repository nos. AG11513 and AG01972; both with the G608G mutation) (http://locus.umdnj.edu/ccr) (3). Fibroblasts from an atypical progeria patient with an R644C substitution in lamin A and fibroblasts from a severe atypical Werner's syndrome patient with an E578V substitution in lamin A were also obtained from Coriell (repository nos. AG00989 and AG04110, respectively) (8). Two potent FTIs, PB-43 and BMS-214662 (14, 16), were used. Unless otherwise noted, cells were treated with a FTI for 48 h at a dose of 2.5 μM, a dose that has little or no effect on cell growth. Untreated cells were incubated with the vehicle DMSO.

Western Blots. Fibroblasts were washed and solubilized with SDS; proteins were separated on 4–12% gradient polyacrylamide gels and then transferred to nitrocellulose membranes for Western blots. The antibody dilutions were 1:5,000 rabbit anti-mouse prelamin A antiserum (an antiserum against a carboxyl-terminal prelamin A peptide, LLGNSSPRSQSSQN; this antibody cannot bind mature lamin A or lamin C) (13, 15), 1:400 anti-lamin A/C mouse IgM monoclonal (lamin A/C monoclonal antibody) (sc-7293, Santa Cruz Biotechnology), 1:400 anti-lamin A/C rabbit IgG (lamin A/C polyclonal antibody) (sc-20680, Santa Cruz Biotechnology), 1:400 anti-lamin A (carboxyl terminus) goat IgG (sc-6214, Santa Cruz Biotechnology), 1:1,000 anti-lamin B (sc-6217, Santa Cruz Biotechnology), 1:1,000 anti-actin goat IgG (sc-1616, Santa Cruz Biotechnology), 1:500 anti-HDJ-2/DNAJ Ab-1 mouse IgG_1 (MS-225-P0, Lab Vision Corporation, Fremont, CA), 1:6,000 horseradish peroxidase (HRP)-labeled anti-goat IgG (sc-2020, Santa Cruz Biotechnology), 1:4,000 HRP-labeled anti-mouse IgM (sc-2064, Santa Cruz Biotechnology), 1:4,000 HRP-labeled anti-mouse Ig (NA931V, Amersham Biosciences), and 1:6,000 HRP-labeled anti-rabbit IgG (NA934V, Amersham Biosciences). Antibody binding was detected with the ECL Plus enhanced chemiluminescence system (Amersham Biosciences) and exposure to x-ray film.

Northern Blots. RNA was extracted from cells with Tri Reagent (Sigma). RNA (5 μg) was size-fractionated on a 1% agarose gel and transferred to a Nytran Supercharge membrane. A ^{32}P-labeled 270-bp probe from the 5′ portion of the *Lmna* cDNA was used to detect prelamin A and lamin C transcripts.

Immunofluoresence Microscopy. Fibroblasts were plated on coverslips at ≈25,000 cells per well in 24-well plates. Fibroblasts were fixed in 3% paraformaldehyde, permeabilized with 0.2% Triton X-100, and blocked with 0.2% BSA/10% FBS. The fibroblasts were incubated for 60 min with antibodies against prelamin A (rabbit anti-mouse prelamin A antiserum) (1:5,000), lamin A (sc-20680, Santa Cruz Biotechnology) (1:200), or lamina-associated protein 2 (LAP2; catalog no. 611001, BD Biosciences, San Jose, CA) (1:400). After being washed, fibroblasts were stained with 1:800 anti-rabbit Cy3-conjugated secondary antibody (catalog no. 711-166-152, Jackson ImmunoResearch), 1:600 anti-mouse Alexa Fluor 488 (A21202, Molecular Probes), and DAPI to visualize DNA. Images were obtained as described in ref. 14. Numbers of normal nuclei (nuclei with a smooth oval shape) and abnormal nuclei (nuclei with blebs, grossly irregular shape, or multiple folds) were counted by two completely blinded observers in cells stained for lamin A or LAP2. Statistical differences were calculated with the χ^2 statistic.

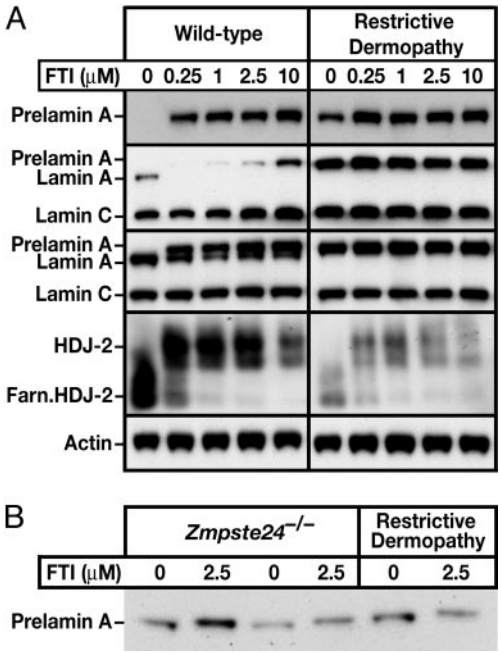

Fig. 1. Western blot analysis of wild-type and RD fibroblasts. (*A*) Western blots of wild-type and RD fibroblasts in the presence and absence of PB-43. Starting from the top gel, the antibodies used were anti-prelamin A, anti-lamin A/C monoclonal, anti-lamin A/C polyclonal, anti-HDJ-2, and anti-actin. (*B*) Western blots of RD fibroblasts and *Zmpste24*$^{-/-}$ MEFs with the prelamin A antibody showing a subtle retardation in the electrophoretic migration of prelamin A in the presence of PB-43.

Results and Discussion

To determine whether the nuclear shape abnormalities in RD fibroblasts could be improved with a FTI, RD and wild-type human fibroblasts (1) were treated with a potent FTI, PB-43. As expected, PB-43 blocked farnesylation in wild-type fibroblasts, as judged by an accumulation of prelamin A and retarded electrophoretic mobility of HDJ-2, a 40-kDa farnesylated *CAAX* protein whose electrophoretic mobility is retarded by blocking farnesylation (Fig. 1*A*). Untreated RD fibroblasts displayed an accumulation of prelamin A and a complete absence of mature lamin A, consistent with *ZMPSTE24* deficiency (4, 5). The FTI treatment did not perturb the total amount of "prelamin A" or "lamin A" in the wild-type or RD fibroblasts (i.e., the amount of prelamin A in FTI-treated fibroblasts was similar to the total amount of lamin A or prelamin A in untreated fibroblasts, as judged by Western blots with lamin A/C antibodies) (Fig. 1*A*). The prelamin A from FTI-treated RD cells migrated slightly more slowly on SDS/polyacrylamide gels than prelamin A from untreated cells (Fig. 1*B*). The slight retardation in electrophoretic mobility was also observed in FTI-treated *Zmpste24*$^{-/-}$ MEFs (Fig. 1*B*). Protein farnesylation increases the electrophoretic mobility of the Ras proteins (17), so the more rapid mobility of prelamin A from untreated RD fibroblasts was not particularly surprising. Also, it is likely that prelamin A in untreated RD fibroblasts is 3 aa shorter than in prelamin A in FTI-treated cells, because the last 3 aa of farnesyl-prelamin A in RD fibroblasts would probably be clipped off by the prenylprotein-specific *CAAX* endoprotease RCE1 (5).

By immunofluorescence microscopy, prelamin A was not detectable in untreated wild-type fibroblasts. In FTI-treated wild-type fibroblasts, however, prelamin A staining was intense and located mainly in the nucleoplasm (Fig. 2*A*). When a lamin A antibody (which binds lamin A and prelamin A but not lamin C) was used, the fluorescence in FTI-treated cells was located mainly in the nucleoplasm (Fig. 2*A*). In untreated RD cells,

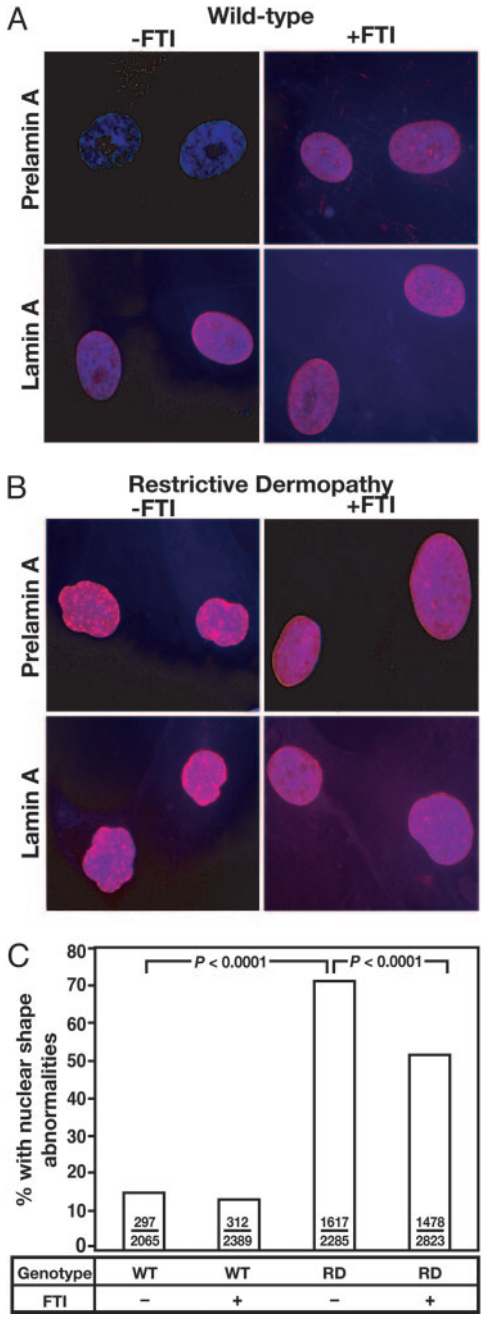

Fig. 2. Effects of a FTI on the localization of prelamin A and on nuclear shape in wild-type and RD fibroblasts. (*A* and *B*) Epifluorescence images showing the effects of the FTI PB-43 on prelamin A and lamin A localization (red) in wild-type (*A*) and RD (*B*) fibroblasts. DNA was visualized with DAPI (blue). In wild-type and RD fibroblasts, the FTI elicited a donut-shaped nuclei in a small percentage of cells (data not shown). (*C*) Frequency of misshapen nuclei in wild-type and RD fibroblasts. Bars show the mean frequency of misshapen nuclei. The number of misshapen nuclei and the total number of nuclei examined are recorded within each bar. The bar graph summarizes data for two independent experiments, but each experiment yielded significant differences ($P < 0.0001$).

prelamin A staining was intense along the nuclear rim and in the nucleoplasm (Fig. 2*B*). After a 48-h incubation with PB-43, prelamin A in RD cells was more evenly distributed in the nucleoplasm; staining at the nuclear rim was less intense but still visible in some cells (Fig. 2*B*). FTI treatment of RD fibroblasts reduced the percentage of fibroblasts with misshapen nuclei (nuclei with blebs, folds, or gross irregularities in shape), as

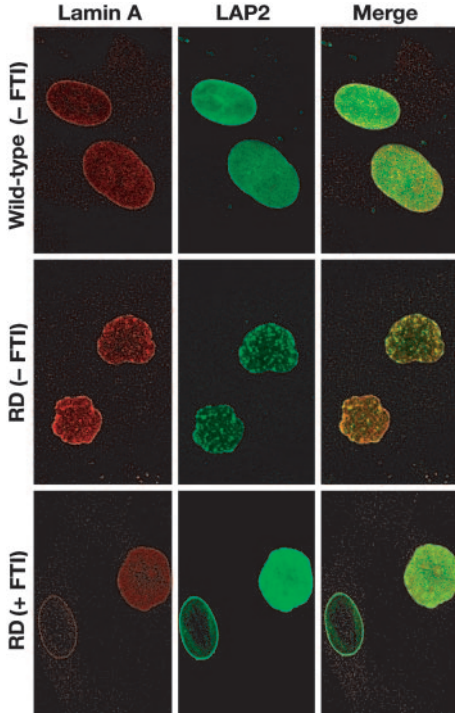

Fig. 3. Confocal images revealing a very irregular distribution of prelamin A (red) and LAP2 (green) (an inner nuclear membrane protein) in the nuclei of untreated RD fibroblasts. After FTI treatment, prelamin A and LAP2 were distributed more evenly in a substantial number of cells.

judged by two observers in two independent experiments ($P < 0.0001$) (Fig. 2*C*). Confocal microscopy of RD cells revealed a strikingly irregular distribution of prelamin A (red) and LAP2 (green) along the nuclear rim and in the nucleoplasm (Fig. 3). In the setting of the FTI, lamin A and LAP2 were distributed more evenly in more than one-half of the RD cells (Fig. 3).

To further explore the impact of FTIs on *Zmpste24*-deficient cells, we examined primary *Zmpste24*$^{-/-}$ and *Zmpste24*$^{+/+}$ MEFs. In wild-type MEFs, a FTI blocked the farnesylation of Hdj-2 and led to an accumulation of prelamin A (Fig. 4*A*). In contrast to results with wild-type human cells, the amount of prelamin A in the FTI-treated wild-type MEFs was lower than the amount of lamin A in untreated MEFs, as judged by Western blots with the lamin A/C antibodies (Fig. 4*A*). The FTI did not perturb lamin C or lamin B1 levels. Similarly, the FTI clearly reduced the amount of prelamin A in *Zmpste24*$^{-/-}$ MEFs, as judged by Western blots with two different lamin A/C antibodies, without affecting lamin C or lamin B1 levels (Fig. 4*A*). Interestingly, the decrease in prelamin A, which was obvious with the lamin A/C antibodies, was not detectable in Western blots using the prelamin A peptide antibody, likely because the peptide antibody against the carboxyl terminus of prelamin A binds nonfarnesylated prelamin A with a higher affinity than farnesylated prelamin A. Virtually identical results were observed with BMS-214662, a different FTI (Fig. 4*B*). We considered the possibility that FTIs reduced prelamin A levels in MEFs by reducing the amount of the prelamin A mRNA; however, Northern blots showed no change in the expression of prelamin A or lamin C (Fig. 4*C*).

By immunofluorescence microscopy, prelamin A was undetectable in wild-type MEFs but was readily detectable in the nucleoplasm of FTI-treated MEFs (Fig. 5*A*). In the absence of a FTI, large amounts of prelamin A were detected at the nuclear rim in *Zmpste24*$^{-/-}$ MEFs (Fig. 5*B*). After a 48-h incubation with a FTI, however, most of the prelamin A was mislocalized to the nucleo-

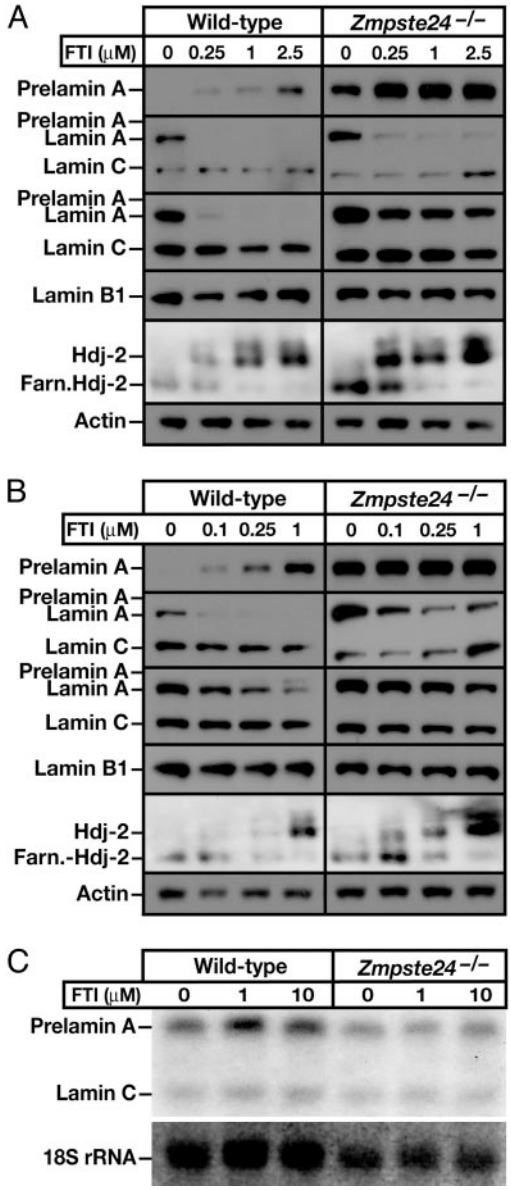

Fig. 4. Analyzing the effects of FTIs on *Zmpste24*$^{-/-}$ MEFs. (*A* and *B*) Western blot analysis of wild-type and *Zmpste24*$^{-/-}$ MEFs in the absence and presence of FTIs PB-43 (*A*) and BMS-214662 (*B*). Starting from the top, the antibodies used were anti-prelamin A, anti-lamin A/C monoclonal, anti-lamin A/C polyclonal, anti-lamin B, anti-HDJ-2, and anti-actin. (*C*) Northern blot analysis of *Zmpste24*$^{-/-}$ MEFs in the absence and presence of PB-43 (1 and 10 μM) with a 5′ *Lmna* probe.

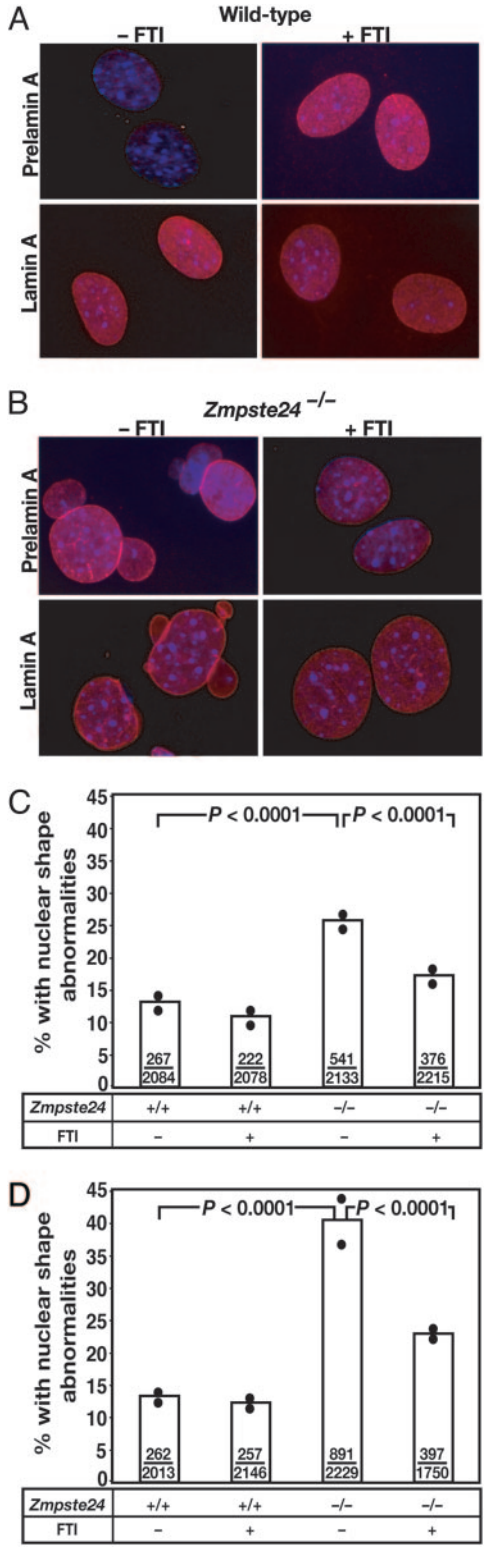

Fig. 5. Effects of a FTI on prelamin A localization and on nuclear shape in *Zmpste24*$^{-/-}$ MEFs. (*A* and *B*) Epifluorescence microscope images showing the effects of PB-43 on prelamin A localization in wild-type (*A*) and *Zmpste24*$^{-/-}$ (*B*) MEFs. Prelamin A and lamin A were visualized with antibodies against prelamin A and lamin A (red); DNA was visualized with DAPI (blue). (*C* and *D*) Frequency of misshapen nuclei in independent experiments with wild-type and *Zmpste24*$^{-/-}$ MEFs in the absence or presence of PB-43. Bars show the mean frequency of misshapen nuclei; the number of misshapen nuclei and total nuclei are recorded within each bar; black circles indicate frequencies for independent cell lines of each genotype.

plasm, and little was located at the nuclear rim (Fig. 5*B*). FTI treatment of *Zmpste24*$^{-/-}$ MEFs led to an unequivocal reduction in misshapen nuclei (mainly nuclei with blebs). In two experiments (each scored by two observers and each involving two independent MEF cell lines of each genotype), the FTI reduced the percentage of *Zmpste24*$^{-/-}$ MEFs with misshapen nuclei ($P < 0.0001$ in both experiments) (Fig. 5 *C* and *D*).

In the human RD cells, the FTI-mediated improvement in nuclear shape occurred in the absence of reduced prelamin A levels in the cell. Thus, we suspect that the favorable effect on the frequency of misshapen nuclei in RD cells was largely due to the partial mislocalization of prelamin A away from the nuclear envelope. In the *Zmpste24*$^{-/-}$ MEFs, the FTI likely improved nuclear shape by dual mechanisms. As in the human RD cells, prelamin A

in the *Zmpste24*$^{-/-}$ MEFs was mislocalized away from the nuclear envelope. However, in addition, the FTI reduced prelamin A levels in *Zmpste24*$^{-/-}$ MEFs. In an earlier study of *Zmpste24*$^{-/-}$ MEFs (15), lowering prelamin A levels by 50% (with a single copy of a *Lmna* knockout allele) dramatically reduced nuclear blebbing.

The fact that FTIs improved nuclear shape in RD fibroblasts and *Zmpste24*$^{-/-}$ MEFs prompted us to determine whether FTIs might improve nuclear shape abnormalities in human HGPS fibroblasts. As judged by Western blots, the FTI had little effect on progerin levels but led to an accumulation of wild-type prelamin A (Fig. 6*A*). After 7 days of FTI treatment, the percentage of HGPS cells with misshapen nuclei was reduced in two different HGPS fibroblast cell lines ($P < 0.0001$ for both) (Fig. 6 *B* and *C*).

As noted earlier, some progeroid syndromes in humans are caused by missense mutations in lamin A, for example R644C and E578V (8). R644C and E578V fibroblasts did not have an accumulation of prelamin A (data not shown) but nevertheless contained misshapen nuclei, presumably because of the structurally and functionally abnormal lamin A. We predicted that a FTI might be effective in improving nuclear shape in the R644C and E578V fibroblasts because the FTI would prevent the biogenesis of mature lamin A and because the nonfarnesylated prelamin A would be located largely in the nucleoplasm. Indeed, the frequency of misshapen nuclei in R644C fibroblasts was reduced with a FTI ($P = 0.0003$ and $P = 0.002$ in two independent experiments) (Fig. 6*D*). Similarly, the frequency of misshapen nuclei in E578V fibroblasts was reduced by the FTI treatment ($P < 0.0001$ in two independent experiments) (Fig. 6*D*).

The missense mutations that we examined, R644C and E578V, are located in the carboxyl terminus of lamin A, a region not shared by lamin C. We thought that it was important to begin with lamin A-specific mutations simply because lamin A biogenesis (and not lamin C synthesis) is affected directly by FTIs. However, mutations causing progeroid syndromes with misshapen nuclei have also been identified within amino acids 1–566, the domain shared by lamin A and lamin C (7, 8). In addition, missense mutations within residues 1–566 cause a host of other "laminopathies," for example, cardiomyopathy with conduction system disease, several forms of muscular dystrophy, partial lipodystrophy, Charcot–Marie–Tooth neuropathy, and mandibuloacral dysplasia (6). Some but not all of the lamin A/C missense mutations cause misshapen nuclei (18). We predict that FTIs will ultimately be shown to improve nuclear shape abnormalities in cells with the lamin A/C missense mutations, because, at the very least, the FTIs would be expected to reduce the amount of mature lamin A reaching the nuclear lamina. One possibility, however, is that the benefit of a FTI would be less impressive with the lamin A/C mutations because the drug would have no direct effect on the mutant lamin C.

Misshapen nuclei, the principal cellular pathology in RD and HGPS, are unequivocally improved by a FTI. The important question is, would a FTI be an effective therapy for lamin-related progeroid syndromes and perhaps for other laminopathies as well? No one knows the answer to this question, but we believe that testing FTIs in *Zmpste24*$^{-/-}$ mice (5) or a gene-targeted mouse model of HGPS (14) is certainly warranted. Also, we believe that it would be reasonable to consider a clinical trial in HGPS patients, particularly given the lethality of the disease and the fact that FTIs are well tolerated oral drugs (19).

We are cautiously optimistic that FTIs would be an effective therapy for human progeroid syndromes simply because it makes intuitive sense that improvements in a "cellular pathology" would ameliorate disease phenotypes at a tissue or organ level. Also, structural abnormalities in the nuclear lamina render fibroblasts more susceptible to apoptosis (20), and it seems likely that cell death underlies some of the disease phenotypes in HGPS. Thus, any pharmacological intervention that improves the integrity of the nuclear lamina might lead to improvements in cell death and disease phenotypes. Another reason for optimism is the fact that the

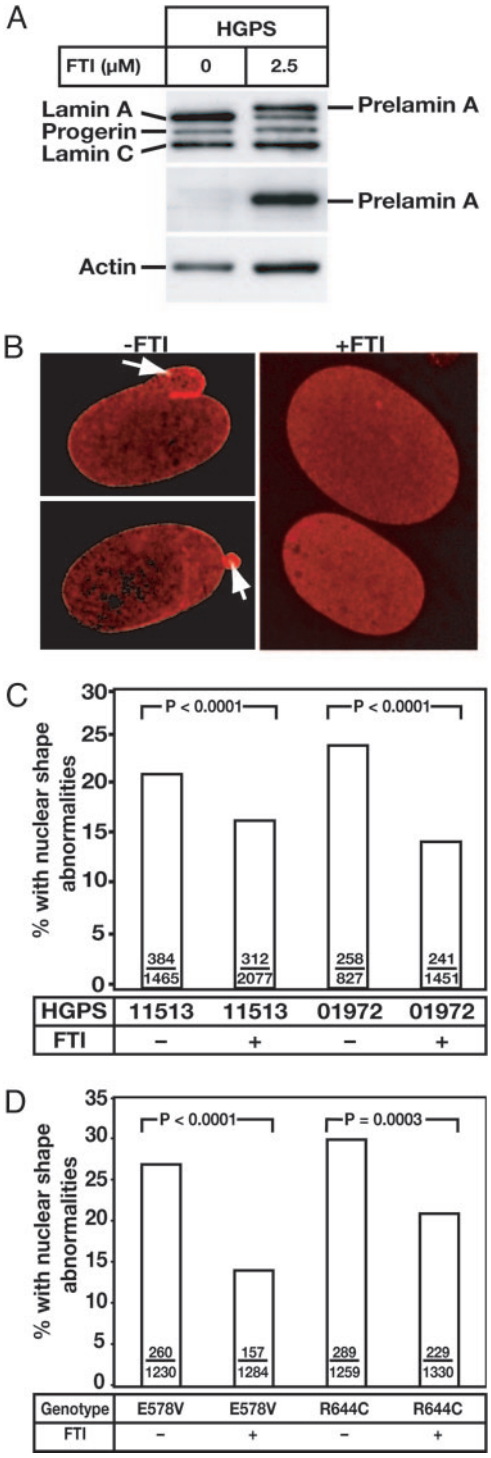

Fig. 6. The effects of a FTI on the frequency of misshapen nuclei in HGPS fibroblasts and fibroblasts from other progeroid syndromes. (*A*) Western blot analysis of HGPS fibroblasts in the absence or presence of PB-43. The antibodies used were anti-lamin A/C polyclonal (top gel), anti-prelamin A (middle gel) and anti-actin (bottom gel). (*B*) Epifluorescence microscope images showing the effects of PB-43 on lamin A (red) localization in human HGPS fibroblasts. The arrows show blebs. (*C*) Impact of a FTI on the frequency of misshapen nuclei in two different HGPS cell lines (AG11513 and AG01972). (*D*) Impact of a FTI on the frequency of misshapen nuclei in fibroblasts with R644C and E578V mutations. Shown is the first of two independent experiments. A second independent observer obtained similar results with statistically significant differences ($P = 0.0059$ for the E578 mutation and $P < 0.0001$ for the R644C mutation). Bars show the mean frequency of misshapen nuclei; the number of misshapen nuclei and total nuclei are recorded within each bar.

nuclear shape and "whole-animal" phenotypes were associated in a recent study of *Zmpste24*$^{-/-}$ mice (15). In that study, lowering prelamin A expression levels by one-half resulted in a parallel reduction in misshapen nuclei and progeria-like disease phenotypes. In addition, striking improvements in disease phenotypes occurred with a mere 50% reduction in farnesyl-prelamin A. Thus, FTIs might be helpful in humans even if the inhibition of farnesyltransferase and the mislocalization of prelamin A were incomplete.

In contrast, a pessimist would argue that some of the disease phenotypes in progeroid disorders could be unrelated to the structural abnormalities in the nuclear envelope. For example, the partial lipodystrophy phenotype might relate in part to perturbed processing of the sterol regulatory element-binding protein transcription factors (21). It is not clear that FTIs would favorably affect every possible disease mechanism, such as altered transcription factor function. In addition, nonfarnesylated prelamin A (or nonfarnesylated progerin) remain structurally abnormal proteins, and we must not forget that minor structural variations in the lamin proteins cause a host of human genetic diseases (6). Thus, nonfarnesylated prelamin A might be toxic and lead to distinct disease phenotypes. In the future, it might be useful to assess the toxicity of nonfarnesylated prelamin A in a gene-targeted mouse model (i.e., by creating a mouse in which the *C* of the *CAAX* motif was changed to a serine).

Bone disease (retarded skeletal growth, micrognathia, osteolytic lesions, and osteoporosis) is a debilitating feature of HGPS (3). If one could merely cure the bone disease in HGPS, it would certainly have a very positive impact on the lives of affected patients. In this regard, we have considered the possibility of bisphosphonate drugs, which are given to millions of people for the treatment of osteoporosis (22). The nitrogen-containing bisphosphonate drugs, all analogues of pyrophosphate, block the activity of farnesyldiphosphate synthase, an enzyme that produces farnesyldiphosphate, a cosubstrate for protein farnesyltransferase (22–24). Blockade of farnesyldiphosphate synthase would be expected to inhibit protein prenylation and cholesterol biosynthesis (22, 24). Indeed, the inhibitory effects of bisphosphonates on protein geranylgeranylation are thought to be important in improving bone density (22, 24). Bisphosphonates bind avidly to bone (22) and are taken up by osteoblasts and osteoclasts, but they have little impact on other tissues.

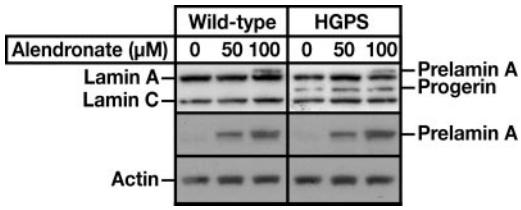

Fig. 7. Western blot analysis of wild-type and HGPS fibroblasts incubated in the presence of alendronate, a bisphosphonate drug, for 3 days. The antibodies used were anti-lamin A/C polyclonal (top gel), anti-prelamin A (middle gel) and anti-actin (bottom gel).

We hypothesized that the bisphosphonate drugs would interfere with the processing of prelamin A to lamin A. Indeed, alendronate (a nitrogen-containing bisphosphonate) partially blocked lamin A biogenesis and led to an accumulation of prelamin A in wild-type and HGPS fibroblasts (Fig. 7). Because bisphosphonates reach high concentrations in bone, it seems quite possible that these drugs would interfere with the farnesylation of progerin in HGPS patients. If so, one could imagine that these drugs could have a favorable impact on the bone disease in HGPS.

Should HGPS patients be treated with bisphosphonates? We would argue, No, not yet. Although these drugs are safe and effective in treating "run-of-the-mill" osteoporosis, their efficacy and safety in HGPS have not been established. Again, testing the impact of these drugs on the osteoporosis and osteolytic lesions of *Zmpste24*$^{-/-}$ mice (5) or HGPS mice (14) would be helpful. Also, we suspect that clinical trials of FTIs in HGPS patients may get off the ground in the next few years, and the interpretation of these trials could be obscured if all of the subjects were taking bisphosphonates. Bisphosphonates are retained in bone for many months or even years, so the presence of these drugs might make it difficult to determine whether FTIs had a favorable effect on bone disease.

We thank Ms. Sandy Chang, Ms. Ellen Fitzmorris, and Ms. Stephanie Young for scoring misshapen nuclei; Mr. Brian Young for assistance with artwork; and Dr. Leslie Gordon for helpful discussions about potential FTI trials in HGPS patients. This work was supported by National Institutes of Health Grants CA099506, AR050200, and AI054384 and a grant from the Progeria Research Foundation.

1. Moulson, C. L., Go, G., Gardner, J. M., van der Wal, A. C., Sillevis Smitt, J. H., van Hagen, J. M. & Miner, J. H. (2005) *J. Invest. Derm.*, in press.
2. Navarro, C. L., Cadinanos, J., De Sandre-Giovannoli, A. D., Bernard, R., Courrier, S., Boccaccio, I., Boyer, A., Kleijer, W. J., Wagner, A., Giuliano, F., *et al*. (2005) *Hum. Mol. Genet.* **14,** 1503–1513.
3. Eriksson, M., Brown, W. T., Gordon, L. B., Glynn, M. W., Singer, J., Scott, L., Erdos, M. R., Robbins, C. M., Moses, T. Y., Berglund, P., *et al*. (2003) *Nature* **423,** 293–298.
4. Pendás, A. M., Zhou, Z., Cadiñanos, J., Freije, J. M. P., Wang, J., Hultenby, K., Astudillo, A., Wernerson, A., Rodríguez, F., Tryggvason, K. & Lopéz-Otín, C. (2002) *Nat. Genet.* **31,** 94–99.
5. Bergo, M. O., Gavino, B., Ross, J., Schmidt, W. K., Hong, C., Kendall, L. V., Mohr, A., Meta, M., Genant, H., Jiang, Y., *et al*. (2002) *Proc. Natl. Acad. Sci. USA* **99,** 13049–13054.
6. Burke, B. & Stewart, C. L. (2002) *Nat. Rev. Mol. Cell. Biol.* **3,** 575–585.
7. Chen, L., Lee, L., Kudlow, B. A., Dos Santos, H. G., Sletvold, O., Shafeghati, Y., Botha, E. G., Garg, A., Hanson, N. B., Martin, G. M., *et al*. (2003) *Lancet* **362,** 440–445.
8. Csoka, A. B., Cao, H., Sammak, P. J., Constantinescu, D., Schatten, G. P. & Hegele, R. A. (2004) *J. Med. Genet.* **41,** 304–308.
9. Corrigan, D. P., Kuszczak, D., Rusinol, A. E., Thewke, D. P., Hrycyna, C. A., Michaelis, S. & Sinensky, M. S. (2005) *Biochem. J.* **387,** 129–138.
10. Hennekes, H. & Nigg, E. A. (1994) *J. Cell Sci.* **107,** 1019–1029.
11. Lutz, R. J., Trujillo, M. A., Denham, K. S., Wenger, L. & Sinensky, M. (1992) *Proc. Natl. Acad. Sci. USA* **89,** 3000–3004.
12. Izumi, M., Vaughan, O. A., Hutchison, C. J. & Gilbert, D. M. (2000) *Mol. Biol. Cell* **11,** 4323–4337.
13. Goldman, R. D., Shumaker, D. K., Erdos, M. R., Eriksson, M., Goldman, A. E., Gordon, L. B., Gruenbaum, Y., Khuon, S., Mendez, M., Varga, R. & Collins, F. S. (2004) *Proc. Natl. Acad. Sci. USA* **101,** 8963–8968.
14. Yang, S. H., Bergo, M. O., Toth, J. I., Qiao, X., Hu, Y., Sandoval, S., Meta, M., Bendale, P., Gelb, M. H., Young, S. G. & Fong, L. G. (2005) *Proc. Natl. Acad. Sci. USA* **102,** 10291–10296.
15. Fong, L. G., Ng, J. K., Meta, M., Cote, N., Yang, S. H., Stewart, C. L., Sullivan, T., Burghardt, A., Majumdar, S., Reue, K., *et al*. (2004) *Proc. Natl. Acad. Sci. USA* **101,** 18111–18116.
16. Laxman, N., Bauer, K. D., Bendale, P., Rivas, R., Yokoyama, K., Hornéy, C. P., Pendyala, P. R., Floyd, D., Lombardo, L. J., Williams, D. K., *et al*. (2005) *J. Med. Chem.* **48,** 3704–3713.
17. Kato, K., Cox, A. D., Hisaka, M. M., Graham, S. M., Buss, J. E. & Der, C. J. (1992) *Proc. Natl. Acad. Sci. USA* **89,** 6403–6407.
18. Muchir, A., Medioni, J., Laluc, M., Massart, C., Arimura, T., van der Kooi, A. J., Desguerre, I., Mayer, M., Ferrer, X., Briault, S., *et al*. (2004) *Muscle Nerve* **30,** 444–450.
19. Alsina, M., Fonseca, R., Wilson, E. F., Belle, A. N., Gerbino, E., Price-Troska, T., Overton, R.M., Ahmann, G., Bruzek, L. M., Adjei, A. A., *et al.* (2004) *Blood* **103,** 3271–3277.
20. Lammerding, J., Schulze, P. C., Takahashi, T., Kozlov, S., Sullivan, T., Kamm, R. D., Stewart, C. L. & Lee, R. T. (2004) *J. Clin. Invest.* **113,** 370–378.
21. Capanni, C., Mattioli, E., Columbaro, M., Lucarelli, E., Parnaik, V. K., Novelli, G., Wehnert, M., Cenni, V., Maraldi, N. M., Squarzoni, S. & Lattanzi, G. (2005) *Hum. Mol. Genet.* **14,** 1489–1502.
22. Rogers, M. J. (2003) *Curr. Pharm. Des.* **9,** 2643–2658.
23. Oades, G. M., Senaratne, S. G., Clarke, I. A., Kirby, R. S. & Colston, K. W. (2003) *J. Urol.* **170,** 246–252.
24. Rogers, M. J. (2004) *Calcif. Tissue Int.* **75,** 451–461.